Biomedical Research and Therapy 2026, 13(03): 8371-8382

Open Access Full Text Article

Original Research

Impact of reoxygenation on Prolyl hydroxylase domain 3 expression and cisplatin sensitivity in breast cancer stem cells after prolonged hypoxia

Nhan Ngo-the Tran[1,*], Khan Dinh Bui[1]

ABSTRACT

Background: Targeting cancer stem cells (CSCs) within the tumor microenvironment has emerged as a critical focus in the development of novel oncological therapies. CSCs are frequently subjected to prolonged hypoxic conditions; while subsequent reoxygenation has been shown to significantly enhance the efficacy of radiotherapy across various cancer cell lines, its impact on chemotherapeutic resistance remains poorly understood. **Methods:** In this study, an *in vitro* model was utilized where breast cancer stem cells were treated with cobalt chloride ($CoCl_2$) for 72 hours to induce hypoxia, followed by a 24-hour incubation in $CoCl_2$-free medium to simulate rapid reoxygenation. Alterations in hypoxia-related gene expression were quantified using RT-qPCR, and changes in BCSC chemoresistance were evaluated via alamarBlue-based IC50 assays. **Results:** Both prolonged hypoxia and rapid reoxygenation significantly modulated the expression of the hypoxia-responsive gene *HIF-1α* and its regulatory target, *PHD3*. Notably, the expression of the drug efflux transporter *ABCG2* was markedly downregulated upon reoxygenation following hypoxic preconditioning. Despite this molecular alteration, the associated reduction in cisplatin resistance did not reach statistical significance. **Conclusion:** Collectively, these findings provide preliminary evidence that integrating oxygen-dependent therapeutics or enhancing oxygen delivery to hypoxic tumor cells influences resistance-associated gene expression, though further optimization is needed to significantly improve chemotherapy efficacy.

Key words: breast cancer stem cells, cell proliferation, cisplatin, drug resistance, hypoxia, prolyl hydroxylase domain 3, reoxygenation

[1]*Stem Cell Institute, University of Science, Ho Chi Minh City, Viet Nam Viet Nam National University Ho Chi Minh City, Viet Nam*

Correspondence

Nhan Ngo-the Tran, Stem Cell Institute, University of Science, Ho Chi Minh City, Viet Nam Viet Nam National University Ho Chi Minh City, Viet Nam

Email: nhantran@sci.edu.vn

History

- Received: Jan 13, 2026
- Accepted: Mar 15, 2026
- Published Online: Mar 31, 2026

DOI : 10.15419/s5qnsv76

INTRODUCTION

In breast cancer, an increasing body of evidence highlights the critical role of cancer stem cells (CSCs) in driving tumor drug resistance[1]. Breast CSCs (BCSCs) are typically identified and isolated based on their distinct $CD44^+/CD24^{-}$/low surface marker phenotype[2]. While various intrinsic mechanisms underlying BCSC therapy resistance have been characterized, the specific contributions of the tumor microenvironment (TME) to treatment failure remain incompletely understood.

Hypoxia is a hallmark feature of the TME[3], and accumulating literature demonstrates a strong association between hypoxic conditions and enhanced therapeutic resistance in CSCs[4]. Consequently, the development of robust *in vitro* hypoxic culture models for CSCs is imperative for the accurate assessment of their chemoresistance profiles. A prevalent method for simulating hypoxia involves treating cells with cobalt chloride ($CoCl_2$)[5,6]. Mechanistically, $CoCl_2$ acts to stabilize hypoxia-inducible factors (HIFs) by inhibiting the activity of prolyl hydroxylase domain (PHD) enzymes across various cancer cell lines[7]. This inhibition leads to the intracellular accumulation of HIFs, thereby triggering cellular responses that effectively recapitulate a hypoxic state[8].

The HIF family consists of three recognized members (HIF-1, HIF-2, and HIF-3). Each functions as a heterodimer comprising an oxygen-labile α subunit (HIF-1α, HIF-2α, or HIF-3α)—which undergoes rapid degradation under normoxic conditions—and a constitutively expressed β subunit, also known as ARNT[9]. Extensive research demonstrates that HIF expression, particularly that of HIF-1, orchestrates numerous physiological and pathological pathways in both normal and malignant tissues[10,11]. Following hypoxia-induced activation, HIF acts as a transcription factor to directly promote angiogenesis and hematopoiesis by upregulating vascular endothelial growth factor (*VEGF*)[12,13] and erythropoietin (*EPO*)[14,15], respectively. Furthermore, HIF has been implicated in augmenting the drug resistance of breast cancer cells under hypoxic stress through

Cite this article : Tran NN, Bui KD. **Impact of reoxygenation on Prolyl hydroxylase domain 3 expression and cisplatin sensitivity in breast cancer stem cells after prolonged hypoxia**. *Biomed. Res. Ther.* 2026; 13(03): 8371-8382.

the upregulation of the ATP-binding cassette subfamily G member 2 (*ABCG2*)[16,17]. Therefore, elucidating the comprehensive regulatory mechanisms governing HIF is crucial for effectively targeting these diverse, HIF-dependent cellular processes.

Prolyl hydroxylase domain (PHD) enzymes serve as primary regulators of HIF stability. Belonging to the prolyl-4-hydroxylase (P4H) protein family, PHD proteins execute post-translational modifications via the hydroxylation of prolyl residues on target proteins, thereby influencing a wide array of physiological processes in metazoans[18–20]. In humans, three principal isoforms exist: PHD1, PHD2, and PHD3[21]. While substantial evidence characterizes PHD3 as a tumor suppressor whose inactivation bolsters cancer cell proliferation under hypoxia[22], conflicting reports suggest that hypoxia-induced PHD3 expression may actively contribute to tumor initiation and progression[23]. Interestingly, *PHD3* retains its functionality under both normoxic and prolonged hypoxic conditions[24]. This sustained activity is driven by a HIF-α–mediated positive feedback loop, wherein HIF-α binds to hypoxia response element (HRE) sequences within the *PHD3* regulatory region[25]. Collectively, these dynamic characteristics position *PHD3* as a highly relevant target in hypoxia-centric cancer research.

Beyond hypoxia, the subsequent restoration of oxygen levels—reoxygenation—has been shown to profoundly impact the trajectory of hypoxic cancer cells. For instance, the sequence of hypoxia followed by reoxygenation induces epithelial-mesenchymal transition (EMT) in colon cancer cells via an NF-κB-dependent signaling pathway[26]. Similarly, in colorectal cancer models, exposure to either extended hypoxia or subsequent reoxygenation stimulates cellular proliferation and confers durable resistance to apoptosis[27]. Although it is evident that both hypoxic and reoxygenation phases dictate cancer cell survival, the precise molecular mechanisms and downstream signaling networks governing these adaptations remain incompletely defined.

To bridge this knowledge gap, the present study utilizes a $CoCl_2$-induced hypoxia model in BCSCs to evaluate the expression dynamics of *PHD3* and associated hypoxia-responsive genes. Ultimately, this research aims to determine how these molecular alterations influence chemotherapeutic resistance following periods of prolonged hypoxia and subsequent rapid reoxygenation.

MATERIALS AND METHODS

Cell Culture

The Vietnamese-derived breast cancer cell line VNBRCA1, originally established in a previous study[28], was obtained from the Cell Bank of the Stem Cell Institute at the University of Science, Vietnam National University Ho Chi Minh City (VNU-HCM). Cells were cultured in Dulbecco's Modified Eagle Medium/Nutrient Mixture F-12 (DMEM/F12; Gibco, USA), supplemented with 10% fetal bovine serum (FBS; Sigma-Aldrich, Germany) and a 1% antibiotic solution (Gibco, USA). The cultures were maintained under normoxic conditions at 37℃ in a humidified incubator containing 5% CO_2. The culture medium was replenished every 48 hours. Upon reaching 70–80% confluence in culture flasks (SPL, Korea), the cells were dissociated using TrypLE Express (1X; Gibco, USA). The resulting cell suspension was centrifuged at 500 × g for 5 minutes, and the cell pellet was reseeded into new culture flasks for continued expansion.

Isolation of Breast Cancer Stem Cells (BCSCs) via Flow Cytometry

VNBRCA1 cells were expanded until the total yield reached approximately 2–3 × 10^7 cells, at which point they were harvested for flow cytometric sorting. The cells were centrifuged at 500 × g for 5 minutes, the supernatant was discarded, and the pellet was resuspended in 210 µL of phosphate-buffered saline (PBS). For the unstained control, a 10 µL aliquot of this suspension was transferred to a 1.5-mL microcentrifuge tube containing 300 µL of PBS. The remaining 200 µL was reserved for antibody labeling. The cells were stained with an allophycocyanin (APC)-conjugated anti-CD44 antibody (SAB4700180; Sigma-Aldrich, Germany) and a fluorescein isothiocyanate (FITC)-conjugated mouse anti-human CD24 antibody (560992; BD Biosciences, USA) at a concentration of 1 µL per 10^6 cells. The samples were incubated in the dark at 4℃ for a minimum of 20 minutes. Following incubation, the cells were centrifuged to remove unbound antibodies, and the pellet was washed with 500 µL of PBS. This washing procedure was repeated twice before the cells were finally resuspended in 1 mL of PBS. Both the control and labeled samples were sorted using a BD FACSMelody™ Cell Sorter (BD Biosciences, USA).

Cells demonstrating the $CD44^+/CD24^{-}$/low phenotype were isolated and subsequently cultured in Human Mammary Epithelial Cell Basal Medium (formerly Medium 171; Gibco, USA) enriched with 1%

Mammary Epithelial Growth Supplement (MEGS; Gibco, USA) and a 1% antibiotic solution (Thermo Fisher Scientific, USA). These cultures were maintained at 37℃ under normoxic, 5% CO_2 conditions. This specific subpopulation has been previously confirmed to possess robust cancer stem cell characteristics[29]. Prior to subsequent downstream assays, the purity and retention of the $CD44^+/CD24^{-}$/low phenotype within the expanded BCSC population were verified via analytical flow cytometry.

Evaluation of Cobalt Chloride ($CoCl_2$) Cytotoxicity for Hypoxia Modeling

To establish a stable hypoxia-mimetic model, a 25 mmol/L stock solution of $CoCl_2$ (Xilong Scientific, China) was prepared. BCSCs were seeded into 96-well plates (SPL, Korea) at a density of 4×10^3 cells per well in 100 µL of medium and allowed 24 hours to adhere. The medium was then replaced with fresh medium containing varying concentrations of $CoCl_2$ (0, 25, 50, 75, 100, 150, 200, and 250 µmol/L). Cellular proliferation and viability were assessed at 24-, 48-, and 72-hour intervals using the alamarBlue assay (Sigma-Aldrich, Germany). Specifically, 10 µL of the alamarBlue reagent was added to each well (final concentration: 10 µg/mL), followed by a 1-hour incubation in the dark. Fluorescence was quantified at an emission wavelength of 590 nm using a DTX880 multimode plate reader (Beckman Coulter, USA). Wells containing only culture medium and the reagent served as blank controls. The percentage of cell proliferation was calculated by subtracting the blank fluorescence from the target readings and normalizing the values against the vehicle control. The mean and standard deviation (SD) for each concentration were derived from three independent biological replicates.

Quantification of *HIF-1α* and *PHD3* mRNA Expression via RT-qPCR

BCSCs were seeded into 6-well plates at a density of 1×10^5 cells per well in 1.5 mL of culture medium. After 24 hours, the control group received fresh medium without $CoCl_2$, while the experimental group was exposed to medium containing 75 µmol/L $CoCl_2$. Cells from both cohorts were harvested at 24, 48, and 72 hours post-treatment, and total RNA was extracted utilizing the easy-BLUE™ Total RNA Extraction Kit (iNtRon Biotechnology, Korea). RNA purity (OD260/OD280 and OD260/OD230 ratios) and concentration were measured using a NanoDrop ND-1000 spectrophotometer (Thermo Fisher Scientific, USA). All reactions were normalized to an input of 100 ng of total RNA. Gene expression profiling was executed using the Luna® Universal One-Step RT-qPCR Kit (New England Biolabs, USA) according to the manufacturer's guidelines. Reverse transcription was performed at 55℃ for 30 minutes using the WarmStart® enzyme system. The qPCR cycling conditions included an initial denaturation at 95℃ for 1 minute, followed by 40 cycles of denaturation at 95℃ for 10 seconds and extension at 60℃ for 30 seconds. The target genes included *β-actin* (forward: 5'- CTGGAACGGTGAAGGTGACA-3'; reverse: 5'-AAGGGACTTCCTGTAACAATGCA-3')[30], which served as a commonly used reference gene for $CoCl_2$–induced hypoxia model[31,32], *HIF-1α* (forward: 5'-TAGCCGAGGAAGAACTATG AAC-3'; reverse: 5'-CTGAGGTTGGTTACTGTTGGTA-3')[33], and *PHD3* (forward: 5'-GCCGGCTGG GCAAATACTA-3'; reverse: 5'-CCGGATAGCAAGCCACCAT-3')[34]. RT-qPCR amplification and data acquisition were performed using a Mastercycler® RealPlex 4 system (Eppendorf, Germany). Cycle threshold (Ct) values were analyzed using the Livak ($2^{-\Delta\Delta Ct}$) method[35]. Melting curve analysis was performed to verify primer specificity.

Assessment of *HIF-1α* Target Gene Expression Under Hypoxia and Reoxygenation

BCSCs were seeded in 6-well plates (1×10^5 cells/well) and allocated into three experimental arms: control, hypoxia, and reoxygenation. Following a 24-hour adherence period, the control group received $CoCl_2$-free medium, whereas the hypoxia and reoxygenation groups were treated with 75 µmol/L $CoCl_2$. At 72 hours, cells in the control and hypoxia groups were harvested. The reoxygenation group was subjected to a washout step and subsequently cultured in $CoCl_2$-free medium for an additional 24 hours to simulate rapid oxygen restoration. Total RNA was extracted from all groups using the easy-BLUE™ Kit. The mRNA expression levels of *HIF-1α*, *PHD3*, *β-actin*, and downstream *HIF-1α* targets, including *VEGF*[36], *EPO*[37], and *ABCG2*[38], were quantified using RT-qPCR as described above.

Determination of Cisplatin Resistance via IC_{50} Assays

A 2.5 mmol/L stock solution of cisplatin (Sigma-Aldrich, Germany) was formulated. BCSCs were seeded into 96-well plates at a density of 4×10^3 cells per well and incubated for 24 hours. The cells were then stratified into control, $CoCl_2$-treated

(hypoxia), and reoxygenation groups. The control group received standard medium, while the remaining two groups received medium containing 75 µmol/L $CoCl_2$. After 72 hours, the reoxygenation group was washed and cultured in standard medium for a further 24 hours. All experimental arms were then exposed to increasing concentrations of cisplatin (0, 1, 5, 25, 100, and 500 µmol/L). Following a 24-hour drug exposure period, cell viability was evaluated using the alamarBlue assay via a DTX880 multimode plate reader. The half-maximal inhibitory concentration (IC_{50}) values for cisplatin were calculated via non-linear regression analysis (log[inhibitor] vs. normalized response) using GraphPad Prism software (version 10.3.1).

Statistical Analysis

All quantitative data are presented as the mean ± standard deviation (SD) derived from a minimum of three independent biological replicates. Flow cytometry data were analyzed and visualized using FlowJo software (version 10.9.1). Differences between two independent groups were evaluated using an unpaired Student's *t*-test, whereas comparisons involving three or more groups were assessed via a one-way analysis of variance (ANOVA) followed by Tukey's post-hoc test. Statistical significance was defined as $p < 0.05$ (*), $p < 0.01$ (**), $p < 0.001$ (***), and $p < 0.0001$ (****). Results with a *p*-value > 0.05 were considered non-significant (ns). All statistical operations and graphical plotting were executed using GraphPad Prism (version 10.3.1).

RESULTS

Isolation and Proliferation of BCSCs

VNBRCA1 cells cultured in DMEM/F12 medium supplemented with 10% FBS and 1% antibiotics exhibited a characteristic epithelial morphology (Figure 1A). Flow cytometric analysis revealed that the $CD44^+/CD24^{-}$/low subpopulation comprised 1.573 ± 1.167% of the total cell population (Figure 1B–D). Following expansion to a yield of 2–3 × 10^7 cells, this $CD44^+/CD24^{-}$/low fraction was isolated and subsequently cultured in M171 medium enriched with 1% MEGS and 1% antibiotics. Post-sorting, these cells adopted an elongated, mesenchymal-like morphology characterized by prominent cluster formation (Figure 1E). The BCSCs were further expanded in M171 medium, and their phenotypic purity was re-evaluated prior to downstream assays. Subsequent flow cytometry confirmed that 93.427 ± 2.935% of the cultured cells successfully retained the targeted $CD44^+/CD24^{-}$/low BCSC phenotype (Figure 1F–H).

Establishment of a $CoCl_2$-Induced Hypoxia Model in BCSCs

To determine the optimal conditions for a prolonged hypoxia model, BCSCs were seeded into 96-well plates and stabilized for 24 hours prior to exposure to varying concentrations of $CoCl_2$ (0, 25, 50, 75, 100, 150, 200, and 250 µmol/L). Cellular viability was assessed over 24, 48, and 72 hours using the alamarBlue assay. Compared to the vehicle control (0 µmol/L), $CoCl_2$ concentrations up to 75 µmol/L did not significantly impair cell viability ($p > 0.05$); however, concentrations at or exceeding 100 µmol/L induced marked cytotoxicity ($p < 0.05$) across all time points (Figure 2A).

Preserving cell viability over a 72-hour exposure period was deemed critical for accurately modeling sustained hypoxia. Given that physiological tissue oxygen levels typically range from 1–5% O_2, allowing cells to remain viable while mounting adaptive hypoxic responses[39], concentrations between 25 and 75 µmol/L were carefully evaluated. Ultimately, 75 µmol/L $CoCl_2$ was identified as the optimal concentration to maximize hypoxia-mimetic signaling while maintaining adequate cell viability.

Subsequent RT-qPCR analysis of BCSCs cultured in 6-well plates and exposed to 75 µmol/L $CoCl_2$ demonstrated significant upregulation of both *HIF-1α* and *PHD3* at 72 hours compared to time-matched controls (*HIF-1α*: 10.62 ± 0.76 vs. 4.53 ± 2.20; *PHD3*: 5.05 ± 2.30 vs. 1.97 ± 0.76; $p < 0.05$). No statistically significant differences in the expression of these genes were observed at the 24- or 48-hour time points (Figure 2B, C). These findings confirm that a 72-hour treatment with 75 µmol/L $CoCl_2$ successfully establishes stable, hypoxia-mimetic conditions in BCSCs.

Expression Dynamics of Hypoxia-Responsive Genes Under Sustained Hypoxia and Reoxygenation

BCSCs were stratified into three experimental cohorts: a normoxic control, a $CoCl_2$-treated group (prolonged hypoxia), and a reoxygenation group. The expression levels of *HIF-1α* and *PHD3*, alongside established downstream targets regulated via hypoxia response elements (*ABCG2*, *VEGF*, and *EPO*), were quantified across all groups. RT-qPCR revealed a significant upregulation of *HIF-1α* and *PHD3* in the $CoCl_2$-treated cohort compared to the normoxic control ($p < 0.05$) , followed by a pronounced downward trend in the reoxygenation group (Figure 3A, B).

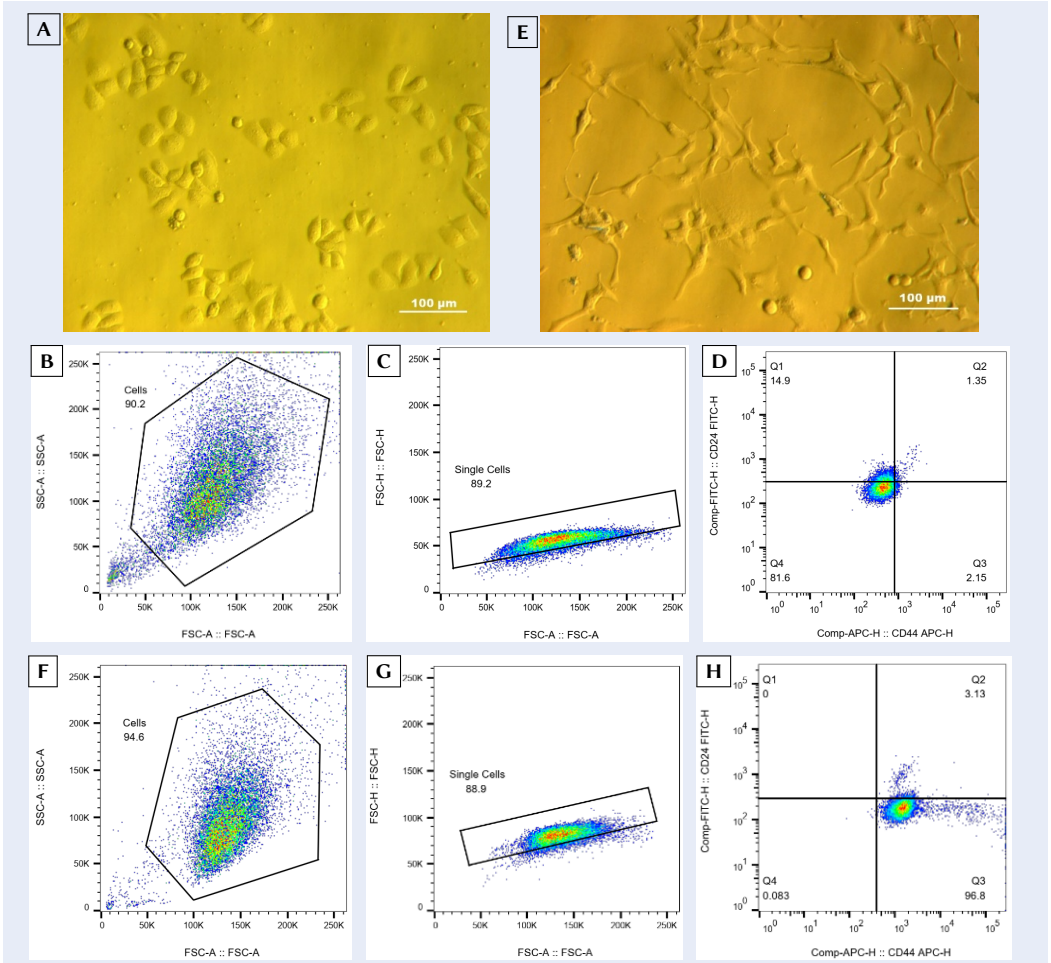

Figure 1: Isolation and stemness validation of breast cancer stem cells (BCSCs) derived from the VNBRCA1 cell line. **(A)** Representative phase-contrast image of VNBRCA1 cells cultured in DMEM/F12 medium supplemented with 10% FBS and 1% antibiotics (Zeiss Axiovert 40 C inverted microscope; Carl Zeiss AG, Germany). **(B)** Initial flow cytometric gating of VNBRCA1 cells identifying a homogeneous event cluster based on forward scatter area (FSC-A: 100K–<250K) and side scatter area (SSC-A: 50K–<250K) parameters. **(C)** Doublet exclusion and single-cell discrimination utilizing FSC-A versus FSC-H gating. **(D)** Quadrant analysis delineating four distinct cell subpopulations: Q1, $CD24^+/CD44^-$; Q2, $CD24^+/CD44^+$; Q3, $CD24^-/CD44^+$ (the target BCSC phenotype); and Q4, $CD24^-/CD44^-$. **(E)** Representative image of the sorted cancer stem cells cultured in M171 medium supplemented with MEGS and 1% antibiotics. **(F)** Re-gating of the expanded BCSCs as a uniform event cluster using FSC-A (100K–<250K) and SSC-A (50K–<250K). **(G)** Confirmation of single-cell gating via FSC-A versus FSC-H analysis. **(H)** Post-expansion quadrant distribution of CD44 and CD24 expression, interpreted as described in panel (D) (n = 3 independent biological replicates).

Similarly, *VEGF* expression mirrored the patterns of *HIF-1α* and *PHD3*, showing a distinct increase under hypoxic conditions and a subsequent decline upon reoxygenation (Figure 3C). Conversely, *ABCG2* and *EPO* exhibited a progressive downregulation from the control to the $CoCl_2$-treated group, reaching their lowest expression levels following reoxygenation (Figure 3D, E). This unexpected suppression of *ABCG2* —a gene critically implicated in cancer cell chemoresistance—prompted further investigation into the functional impact of these culture conditions on BCSC cisplatin sensitivity.

Evaluation of Cisplatin Resistance Across Culture Conditions

To assess chemoresistance functionally, BCSCs were seeded in 96-well plates, subjected to the three aforementioned culture conditions, and subsequently treated with increasing doses of cisplatin (0 to 500 µmol/L). Following 24 hours of drug expo-

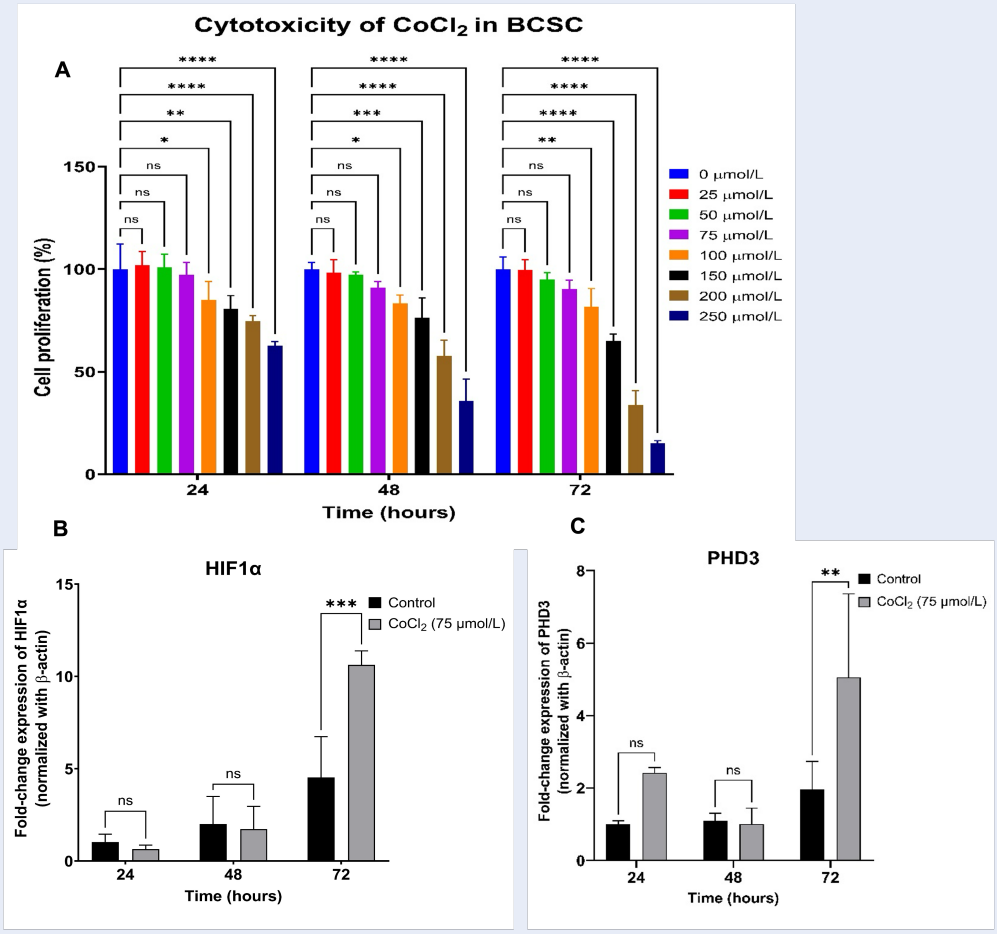

Figure 2: Establishment of a cobalt chloride ($CoCl_2$)-induced hypoxia model. (A) Cytotoxic effects of $CoCl_2$ on BCSCs treated with concentrations ranging from 0 to 250 µmol/L (0, 25, 50, 75, 100, 150, 200, and 250 µmol/L) evaluated at 24, 48, and 72 hours post-treatment. **(B)** Relative mRNA expression of *HIF-1α* in BCSCs exposed to 75 µmol/L $CoCl_2$ at 24, 48, and 72 hours. **(C)** Relative mRNA expression of *PHD3* in BCSCs exposed to 75 µmol/L $CoCl_2$ at 24, 48, and 72 hours. Data are presented as the mean ± SD derived from at least three independent biological replicates (n = 3). Statistical significance is denoted as follows: ns, not significant ($p > 0.05$); *, $p < 0.05$; **, $p < 0.005$; ***, $p < 0.001$; and ****, $p < 0.0001$.

sure, relative cell survival was quantified. The calculated cisplatin IC_{50} values for the control, $CoCl_2$-treated, and reoxygenation groups were 122.2 ± 35.59 µmol/L, 99.44 ± 36.79 µmol/L, and 66.45 ± 26.38 µmol/L, respectively (Figure 4). Despite the observed trend toward increased cisplatin sensitivity in the reoxygenation group, one-way ANOVA indicated that these differences did not reach statistical significance among the three cohorts.

DISCUSSION

Cancer cells exhibiting a $CD44^+/CD24^{-}$/low phenotype isolated from breast tumors possess well-documented stem cell-like properties[40]. Similarly, side-population cells with this specific phenotype derived from the VNBRCA1 breast cancer cell line have been reported to display defining cancer stem cell (CSC) features, including tumor initiation capacity, drug resistance, and metastatic potential[29]. Consistent with these established findings, the present study successfully isolated and maintained $CD44^+/CD24^{-}$/low cells to serve as a targeted experimental model for breast cancer stem cells (BCSCs). Cobalt chloride ($CoCl_2$) is widely utilized as a chemical hypoxia-mimetic agent[41]. This compound upregulates HIF-1α via both transcriptional and translational mechanisms[42]. Conversely, HIF-1α enhances *PHD3* expression during sustained hypoxia by binding to the hypoxia-response element (HRE) within the *PHD3* promoter[43]. Furthermore, previ-

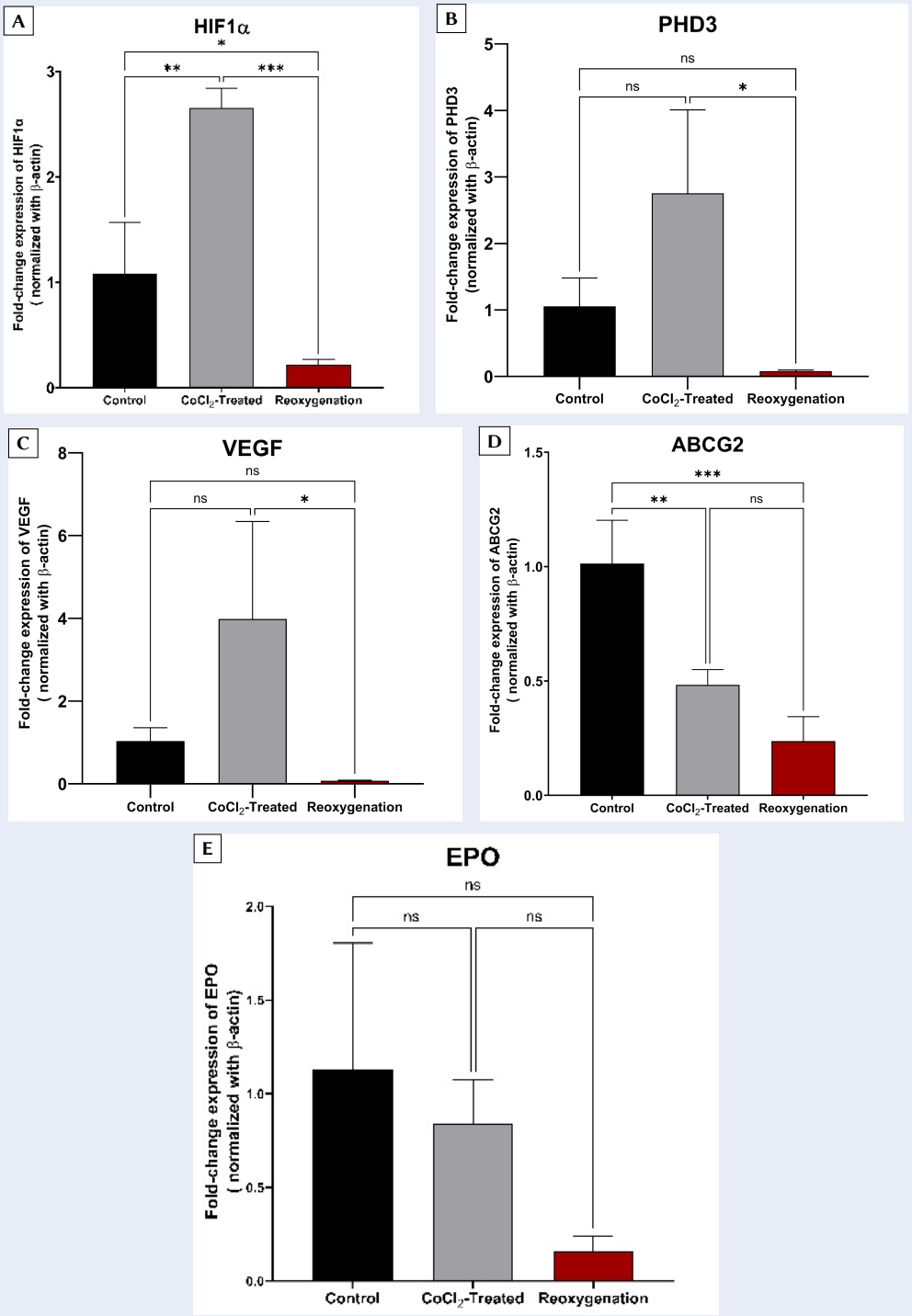

Figure 3: **Fold-change expression of target genes across the three experimental groups.** The experimental cohorts included: a control group (non-$CoCl_2$-treated); a $CoCl_2$-treated group (cells exposed to 75 µmol/L $CoCl_2$ for 24 h); and a reoxygenation group (cells treated with 75 µmol/L $CoCl_2$ for 24 h, followed by culture in $CoCl_2$-free medium for an additional 24 h). Relative mRNA fold-change expression is shown for: **(A)** *HIF-1α*; **(B)** *PHD3*; **(C)** *VEGF*; **(D)** *ABCG2*; and **(E)** *EPO*. Data are presented as the mean ± SD derived from at least three independent biological replicates (n = 3). Statistical significance is denoted as follows: ns, not significant ($p > 0.05$); *, $p < 0.05$; **, $p < 0.005$; ***, $p < 0.001$; and ****, $p < 0.0001$.

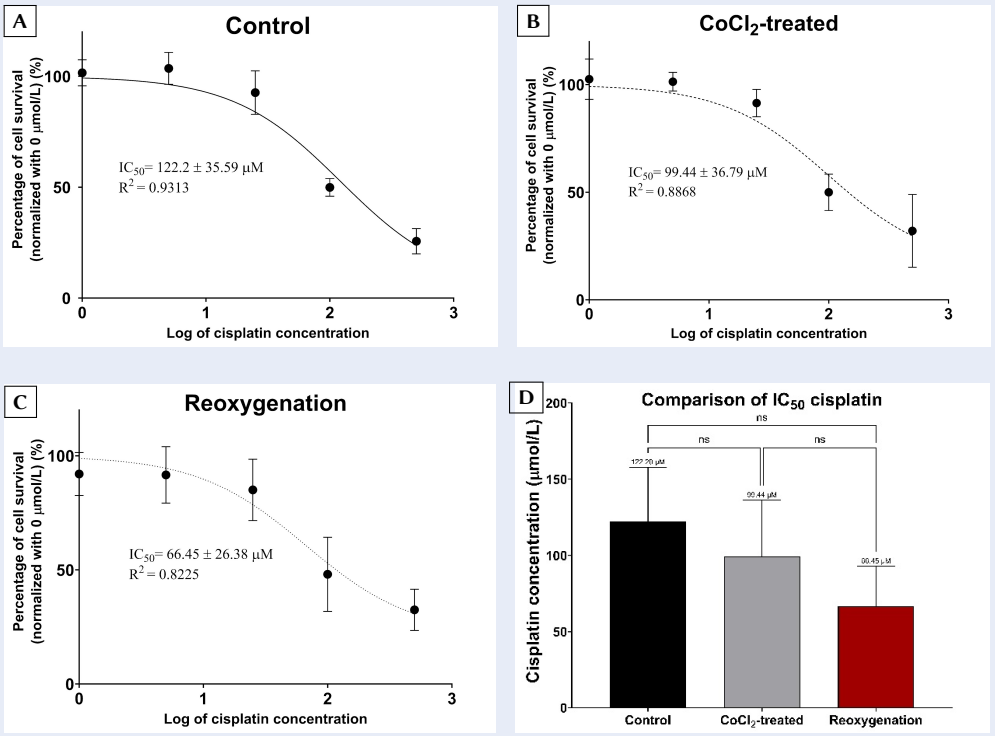

Figure 4: Evaluation of cisplatin resistance in BCSCs across the three experimental groups. The IC_{50} values for cisplatin were determined in the control (non-$CoCl_2$-treated), $CoCl_2$-treated (cells exposed to 75 µmol/L $CoCl_2$ for 24 h), and reoxygenation groups (cells treated with 75 µmol/L $CoCl_2$ for 24 h followed by culture in $CoCl_2$-free medium for an additional 24 h). **(A)** Control group; **(B)** $CoCl_2$-treated group; and **(C)** Reoxygenation group. **(D)** Comparison of the calculated IC_{50} values among the three experimental cohorts. Data are presented as the mean ± SD derived from at least three independent biological replicates (n = 3). Statistical significance is denoted as follows: ns, not significant ($p > 0.05$); *, $p < 0.05$; **, $p < 0.005$; ***, $p < 0.001$; and ****, $p < 0.0001$.

ous literature demonstrates that the optimal $CoCl_2$ concentration for inducing hypoxia is highly dependent on the specific cancer cell line utilized[7,44]. In the current study, the maximal induction of both *HIF-1α* and *PHD3* was observed following a 72-hour treatment with 75 µmol/L $CoCl_2$. Consequently, these optimized parameters were employed to establish a robust prolonged hypoxia model. However, it is imperative to note that $CoCl_2$ may exert off-target effects independent of canonical hypoxic signaling pathways. Cobalt ions are known to induce oxidative stress[45], disrupt mitochondrial function[46], and perturb other metal-sensitive cellular mechanisms[47–49], all of which could potentially confound interpretations specific to true hypoxia. Accordingly, findings derived from $CoCl_2$-based models should be interpreted with caution and warrant future validation using physiological hypoxia systems, such as specialized hypoxia chambers.

Reoxygenation entails the resupply of oxygen to cells or tissues following a period of oxygen deprivation[50]. While this phenomenon is frequently associated with ischemia-reperfusion cellular injury[51], reoxygenation within the context of cancer research has also been shown to exert profound effects on cancer cell biology and radiotherapy outcomes[52,53]. Its specific role in modulating the chemoresistance of hypoxic cancer cells, however, remains incompletely elucidated. Nevertheless, some previous studies indicate that restoring oxygen to hypoxic, drug-resistant tumor cells can potentially reverse their resistance profiles, thereby re-sensitizing them to anticancer therapeutics[54,55]. To evaluate the impact of reoxygenation on CSC drug resistance in our model, BCSCs subjected to prolonged $CoCl_2$ treatment were subsequently cultured in $CoCl_2$-free medium to simulate a rapid reoxygenation event.

Gene expression profiling revealed that *HIF-1α*, *PHD3*, and *VEGF* exhibited parallel expression tra-

jectories: elevated levels under hypoxic conditions followed by a sharp decline upon reoxygenation. This trend likely reflects the rapid degradation and downregulation of HIF-1α during reoxygenation, which subsequently curtails the transcription of its downstream targets, *VEGF* and *PHD3*. In contrast, the expression of the erythropoiesis-associated gene *EPO* remained relatively stable across both the $CoCl_2$-treated and reoxygenation groups. This stability may be attributed to the fact that *EPO* is predominantly regulated by HIF-2α[56,57], rather than HIF-1α.

Notably, the expression of the drug efflux transporter *ABCG2* decreased significantly from the normoxic control group to the $CoCl_2$-treated group. This hypoxia-induced downregulation contrasts with the established role of ABCG2 in mediating chemoresistance in breast cancer cells[58–60]. Consistent with our findings, a study focusing on pancreatic cancer also reported a significant reduction in *ABCG2* expression under both acute and chronic hypoxic conditions[61]; however, that study primarily cataloged chemoresistance-related gene variations without delving deeply into the underlying molecular mechanisms. Additional investigations utilizing the BeWo placental cell line and human fetal brain endothelial cells have similarly demonstrated *ABCG2* downregulation under hypoxic stress[62,63]. Collectively, these observations suggest that hypoxia may uniquely and negatively regulate *ABCG2* in certain sensitive cell types, particularly those exhibiting pronounced stem-like characteristics.

Upon reoxygenation, *ABCG2* expression remained markedly lower than in the control group ; however, no significant difference was observed relative to the $CoCl_2$-treated cohort. This pattern implies that rapid reoxygenation following a prolonged hypoxic period may be insufficient to immediately reverse hypoxia-induced transcriptional alterations, and it may concurrently exert a negative impact on cell viability. Furthermore, the reduction in *ABCG2* expression without a corresponding, statistically significant increase in cisplatin sensitivity underscores a highly complex regulatory landscape governing chemoresistance. While a decrease in the cisplatin IC_{50} from the control to the reoxygenation group was observed, the difference failed to reach statistical significance. A post hoc power analysis suggested that the current sample size may have been underpowered to detect modest intergroup differences. The substantial variability noted in the cisplatin dose–response curves likely reflects inherent biological heterogeneity within the BCSC subpopulation, intrinsic assay variability, and the limited number of biological replicates (n = 3). Accordingly, these IC_{50} results should be considered preliminary and require validation in larger-scale studies.

Several limitations of the present study must be acknowledged. First, the utilization of $CoCl_2$ as a hypoxia mimetic, rather than employing specialized systems to generate physiological hypoxia, may elicit distinct cellular responses due to differing mechanisms of action. Second, additional protein-level validation of the analyzed mRNA targets, particularly HIF-1α and PHD3, is necessary to confirm that these transcriptional changes translate proportionally to the functional protein level. A critical limitation is the omission of HIF-2α assessment. While HIF-1α acts as a principal mediator of the acute hypoxic response, HIF-2α regulates a partially distinct transcriptional program critically implicated in stemness, erythropoietic signaling, and therapy resistance. The absence of HIF-2α data, therefore, restricts a fully comprehensive interpretation of hypoxia-driven regulatory networks in BCSCs. Future studies should incorporate parallel transcript- and protein-level analyses of HIF-2α to delineate isoform-specific roles and bolster the mechanistic framework. Another methodological challenge is the inherent difficulty in maintaining the highly plastic $CD44^+/CD24^-$/low stem-like phenotype over prolonged culture periods ; nevertheless, surface marker expression was rigorously verified across each experimental replicate in this study. Finally, the exclusive reliance on a single, local cell line (VNBRCA1) limits the broader generalizability of these findings across diverse breast cancer subtypes.

CONCLUSION

This study successfully isolated and enriched a distinct subpopulation of breast cancer cells characterized by a $CD44^+/CD24^-$/low cancer stem-like phenotype. The application of 75 μmol/L $CoCl_2$ over a 72-hour period effectively established a robust, prolonged hypoxia-mimetic *in vitro* model. The induction of hypoxia in these breast cancer stem cells (BCSCs), followed by rapid reoxygenation via medium replacement, led to a marked downregulation of the drug efflux transporter *ABCG2*. However, this observed molecular alteration did not translate into a statistically significant enhancement in cisplatin sensitivity. Collectively, these findings indicate that the dynamic modulation of tumor oxygenation may influence the chemotherapeutic response

profile of hypoxic cancer stem cells. Nevertheless, further comprehensive investigations exploring downstream hypoxia-responsive targets, particularly *EPO*, are essential to fully elucidate the complex underlying molecular mechanisms governing these cellular adaptations.

ABBREVIATIONS

ABCG2: ATP binding cassette subfamily G member 2; **ANOVA**: Analysis of variance; **ARNT**: Aryl hydrocarbon receptor nuclear translocator; **BCSCs**: Breast cancer stem cells; **bHLH**: basic helix-loop-helix; **CD24**: cluster of differentiation 24; **CD44**: cluster of differentiation 44; **DMEM/F12**: Dulbecco's modified Eagle's medium: nutrient mixture F12; **EMT**: epithelial–mesenchymal transition; **EPO**: Erythropoietin; **HIF-1α**: hypoxia-inducible factor 1 alpha; **HRE**: hypoxia response element; **MEGS**: Mammary Epithelial Growth Supplement; **PAS**: PER-ARNT-SIM; **PER**: Period protein; **PHD3**: prolyl hydroxylase domain 3; **SIM**: Single-minded; **TME**: tumor microenvironment; **VEGF**: Vascular endothelial growth factor.

ACKNOWLEDGMENTS

None.

AUTHOR'S CONTRIBUTIONS

Nhan Ngo-The Tran and Khan Dinh Bui contributed equally to all aspects of this work. Nhan Ngo-The Tran was primarily responsible for experimental design and execution. Khan Dinh Bui provided critical feedback and detailed revisions for the manuscript.

FUNDING

This research is funded by University of Science, VNU-HCM under grant number T2023-80.

AVAILABILITY OF DATA AND MATERIALS

Data and materials used and/or analyzed during the current study are available from the corresponding author on reasonable request.

ETHICS APPROVAL AND CONSENT TO PARTICIPATE

Not applicable.

CONSENT FOR PUBLICATION

Not applicable.

DECLARATION OF GENERATIVE AI AND AI-ASSISTED TECHNOLOGIES IN THE WRITING PROCESS

The authors declare that they have used generative AI and/or AI-assisted technologies in the writing process before submission, but only to improve the language and readability of their paper.

COMPETING INTERESTS

The authors declare that they have no competing interests.

REFERENCES

1. Zheng Q, Zhang M, Zhou F, Zhang L, Meng X. The Breast Cancer Stem Cells Traits and Drug Resistance. Front Pharmacol. 2021 Jan;11:599965. PMID: 33584277. Available from: https://doi.org/10.3389/fphar.2020.599965.
2. DA Cruz Paula A, Lopes C. Implications of Different Cancer Stem Cell Phenotypes in Breast Cancer. Anticancer Res. 2017 May;37(5):2173–2183. PMID: 28476780. Available from: https://doi.org/10.21873/anticanres.11552.
3. Najafi M, Farhood B, Mortezaee K, Kharazinejad E, Majidpoor J, Ahadi R. Hypoxia in solid tumors: a key promoter of cancer stem cell (CSC) resistance. J Cancer Res Clin Oncol. 2020 Jan;146(1):19–31. PMID: 31734836. Available from: https://doi.org/10.1007/s00432-019-03080-1.
4. Sun X, Lv X, Yan Y, Zhao Y, Ma R, He M, et al. Hypoxia-mediated cancer stem cell resistance and targeted therapy. Biomed Pharmacother. 2020 Oct;130:110623. PMID: 32791395. Available from: https://doi.org/10.1016/j.biopha.2020.110623.
5. Barton A, Jaśkiewicz M, Więch-Walów A, Moszyńska A, Cabaj A, Wielockx B, et al. Challenges in mimicking hypoxia: insights into HIF-regulated MiRNA expression induced by DMOG and $CoCl_2$. Cell Commun Signal. 2025 Oct;23(1):454. PMID: 41126276. Available from: https://doi.org/10.1186/s12964-025-02459-7.
6. Wang Y, Zhao J, Sun L, Xu D, Wei X, Li J, et al. Resveratrol attenuates the $CoCl_2$-induced hypoxia damage by regulation of lysine β-hydroxybutyrylation in PC12 cells. BMC Neurol. 2025 Apr;25(1):153. PMID: 40211144. Available from: https://doi.org/10.1186/s12883-025-04171-y.
7. Khakshour E, Bahreyni-Toossi MT, Anvari K, Shahram MA, Vaziri-Nezamdoust F, Azimian H. Evaluation of the effects of simulated hypoxia by $CoCl_2$ on radioresistance and change of hypoxia-inducible factors in human glioblastoma U87 tumor cell line. Mutat Res. 2024;828:111848. PMID: 38154290. Available from: https://doi.org/10.1016/j.mrfmmm.2023.111848.
8. Navarrete-Anastasio G, Orozco-Ibarra M, Silva-Palacios A. A Brief Description of the Cellular Mechanisms Involved in Cardiac Chemical Hypoxia. Cardiovasc Toxicol. 2026 Jan;26(2):18. PMID: 41563660. Available from: https://doi.org/10.1007/s12012-026-10091-1.
9. Wu D, Potluri N, Lu J, Kim Y, Rastinejad F. Structural integration in hypoxia-inducible factors. Nature. 2015 Aug;524(7565):303–308. PMID: 26245371. Available from: https://doi.org/10.1038/nature14883.
10. Zhao Y, Xing C, Deng Y, Ye C, Peng H. HIF-1α signaling: essential roles in tumorigenesis and implications in targeted therapies. Genes Dis. 2023 Mar;11(1):234–251. PMID: 37588219. Available from: https://doi.org/10.1016/j.gendis.2023.02.039.
11. Basheeruddin M, Qausain S. Hypoxia-Inducible Factor 1-Alpha (HIF-1α): An Essential Regulator in Cellular Metabolic Control. Cureus. 2024 Jul;16(7):e63852. PMID: 39099978. Available from: https://doi.org/10.7759/cureus.63852.

12. Lei Z, Luo Y, Lu J, Fu Q, Wang C, Chen Q, et al. FBXO22 promotes HCC angiogenesis and metastasis via RPS5/AKT/HIF-1α/VEGF-A signaling axis. Cancer Gene Ther. 2025 Feb;32(2):198–213. PMID: 39809956. Available from: https://doi.org/10.1038/s41417-024-00861-w.
13. Acuña-Pilarte K, Koh MY. The HIF axes in cancer: angiogenesis, metabolism, and immune-modulation. Trends Biochem Sci. 2025 Aug;50(8):677–694. PMID: 40640048. Available from: https://doi.org/10.1016/j.tibs.2025.06.005.
14. Zimolova V, Lorenzo F, Yang C, Korinek V, Prchal J, Lanikova L. Modeling autosomal dominant erythrocytosis due HIF-2α E398K mutation reveals novel mechanism of erythropoiesis control. Blood. 2025;146(Supplement 1):2891. Available from: https://doi.org/10.1182/blood-2025-2891.
15. Yang L, Luo Z, Wang S, Lin J, Chen Y, Wu Y. Roxadustat induces erythroid differentiation of erythroleukemia cells through the hypoxia inducible factor-α/GATA binding protein 1 axis. Cell Signal. 2026 Mar;139:112340. PMID: 41443284. Available from: https://doi.org/10.1016/j.cellsig.2025.112340.
16. Nath SD, Hossain Tanim MT, Akash MM, Golam Mostafa M, Sajib AA. Co-expression of HIF1A with multi-drug transporters (P-GP, MRP1, and BCRP) in chemoresistant breast, colorectal, and ovarian cancer cells. J Genet Eng Biotechnol. 2025 Jun;23(2):100496. PMID: 40390503. Available from: https://doi.org/10.1016/j.jgeb.2025.100496.
17. Zhu X, Liu T, Yin X. TMEM158, as plasma cfRNA marker, promotes proliferation and doxorubicin resistance in ovarian cancer. Pharmacogenomics J. 2024 Nov;24(6):34. PMID: 39543089. Available from: https://doi.org/10.1038/s41397-024-00357-8.
18. Wu F, Liu Q, Zhang J, Xu D, Jiang X, Zhang K, et al. Prolyl 4-hydroxylase subunit alpha-2 acts as a TRIM21 ubiquitination substrate to promote papillary thyroid cancer progression via the glycolytic pathway. Cell Death Dis. 2025 May;16(1):395. PMID: 40379610. Available from: https://doi.org/10.1038/s41419-025-07702-0.
19. Najar Hasson S, Kilimnik I, Shahar B, Lifshits LA, Sova M, Bar DZ, et al. Prolyl-hydroxylase domain inhibition enhances collagen levels in oral mucosa-derived fibroblasts. Biochim Biophys Acta Mol Basis Dis. 2026 Mar;1872(3):168124. PMID: 41319981. Available from: https://doi.org/10.1016/j.bbadis.2025.168124.
20. Lin Y, Chen P, Wu Z, Jiang W, Han D, Mai K, et al. Proline promotes prolyl 4-hydroxylase subunit alpha 1 via transforming growth factor beta 1 to increase the synthesis and deposition of collagen in grass carp (Ctenopharyngodon idellus) muscle fibroblasts: insights from integrated bioinformatics and functional analysis. Anim Nutr. 2026 Jan;24:109–120. PMID: 41704244. Available from: https://doi.org/10.1016/j.aninu.2025.06.014.
21. Hou Y, Zhang ZH, Li WQ, Han GX, Shen K, Xie YB. Prolyl hydroxylase domain proteins: Localization, regulation, function and their role in erythropoiesis (Review). Mol Med Rep. 2026 Mar;33(3):82. PMID: 41543162. Available from: https://doi.org/10.3892/mmr.2026.13792.
22. Zhou P, Peng X, Tang S, Zhang K, Tan Z, Li D, et al. E3 ligase MAEA-mediated ubiquitination and degradation of PHD3 promotes glioblastoma progression. Oncogene. 2023 Apr;42(16):1308–1320. PMID: 36882523. Available from: https://doi.org/10.1038/s41388-023-02644-3.
23. Chu X, Xiang M, Feng L, Liu H, Zhou C. Prolyl hydroxylase 3 involvement in lung cancer progression under hypoxic conditions: association with hypoxia-inducible factor-1α and pyruvate kinase M2. J Thorac Dis. 2019 Sep;11(9):3941–3950. PMID: 31656668. Available from: https://doi.org/10.21037/jtd.2019.08.124.
24. Jaakkola PM, Rantanen K. The regulation, localization, and functions of oxygen-sensing prolyl hydroxylase PHD3. Biol Chem. 2013 Apr;394(4):449–457. PMID: 23380539. Available from: https://doi.org/10.1515/hsz-2012-0330.
25. Henze AT, Riedel J, Diem T, Wenner J, Flamme I, Pouyseggur J, et al. Prolyl hydroxylases 2 and 3 act in gliomas as protective negative feedback regulators of hypoxia-inducible factors. Cancer Res. 2010 Jan;70(1):357–366. PMID: 20028863. Available from: https://doi.org/10.1158/0008-5472.CAN-09-1876.
26. Okajima M, Kokura S, Ishikawa T, Mizushima K, Tsuchiya R, Matsuyama T, et al. Anoxia/reoxygenation induces epithelial-mesenchymal transition in human colon cancer cell lines. Oncol Rep. 2013 Jun;29(6):2311–2317. PMID: 23589103. Available from: https://doi.org/10.3892/or.2013.2401.
27. Kinoshita M, Johnson DL, Shatney CH, Lee YL, Mochizuki H. Cancer cells surviving hypoxia obtain hypoxia resistance and maintain anti-apoptotic potential under reoxygenation. Int J Cancer. 2001 Feb;91(3):322–326. PMID: 11169954. Available from: https://doi.org/10.1002/1097-0215(200002)9999:9999<::AID-IJC1064>3.0.CO;2-P.
28. Phuc PV, Trung LT, Nhung TH, Tue VG, Thuy DT, Ngoc PK. Isolation of cancer cell line from woman breast tumor. Vietnam J Biotechnol. 2010;8(4):1775–1783.
29. Phuc PV, Khuong TT, Dong LV, Kiet TD, Giang TT, Ngoc PK. Isolation and characterization of breast cancer stem cells from malignant tumours in Vietnamese women. J Cell Anim Biol. 2010;4(12):163–169.
30. Weber R, Bertoni AP, Bessestil LW, Brasil BM, Brum LS, Furlanetto TW. Validation of reference genes for normalization gene expression in reverse transcription quantitative PCR in human normal thyroid and goiter tissue. BioMed Res Int. 2014;2014:198582. PMID: 24900955. Available from: https://doi.org/10.1155/2014/198582.
31. Rana NK, Singh P, Koch B. $CoCl_2$ simulated hypoxia induce cell proliferation and alter the expression pattern of hypoxia associated genes involved in angiogenesis and apoptosis. Biol Res. 2019 Mar;52(1):12. PMID: 30876462. Available from: https://doi.org/10.1186/s40659-019-0221-z.
32. Dai ZJ, Gao J, Ma XB, Yan K, Liu XX, Kang HF, et al. Up-regulation of hypoxia inducible factor-1α by cobalt chloride correlates with proliferation and apoptosis in PC-2 cells. J Exp Clin Cancer Res. 2012 Mar;31(1):28. PMID: 22453051. Available from: https://doi.org/10.1186/1756-9966-31-28.
33. Hussein NA, Rashad MM, Abdou AS, Hussein AM, Mohamed HM. Gene profiling of SEC13, SMAD7, GHRL, long non-coding RNA GHRLOS, HIF-1α in gastric cancer patients. Sci Rep. 2022 Apr;12(1):6555. PMID: 35449150. Available from: https://doi.org/10.1038/s41598-022-10402-w.
34. Bialesova L, Xu L, Gustafsson J, Haldosen LA, Zhao C, Dahlman-Wright K. Estrogen receptor β2 induces proliferation and invasiveness of triple negative breast cancer cells: association with regulation of PHD3 and HIF-1α. Oncotarget. 2017 Sep;8(44):76622–76633. PMID: 29100336. Available from: https://doi.org/10.18632/oncotarget.20635.
35. Livak KJ, Schmittgen TD. Analysis of relative gene expression data using real-time quantitative PCR and the 2(-Delta Delta C(T)) Method. Methods. 2001 Dec;25(4):402–408. PMID: 11846609. Available from: https://doi.org/10.1006/meth.2001.1262.
36. Yun H, Lee M, Kim SS, Ha J. Glucose deprivation increases mRNA stability of vascular endothelial growth factor through activation of AMP-activated protein kinase in DU145 prostate carcinoma. J Biol Chem. 2005 Mar;280(11):9963–9972. PMID: 15640157. Available from: https://doi.org/10.1074/jbc.M412994200.
37. Winter SC, Shah KA, Campo L, Turley H, Leek R, Corbridge RJ, et al. Relation of erythropoietin and erythropoietin receptor expression to hypoxia and anemia in head and neck squamous cell carcinoma. Clin Cancer Res. 2005 Nov;11(21):7614–7620. PMID: 16278379. Available from: https://doi.org/10.1158/1078-0432.CCR-05-1097.
38. Shek AB, Kurbanov RD, Alieva RB, Abdullaeva GJ, Nagay AV, Abdullaev AA, et al. Personalized rosuvastatin therapy in problem patients with partial statin intolerance. Arch Med Sci Atheroscler Dis. 2018 Jun;3(1):e83–e89. PMID: 30775595. Available from: https://doi.org/10.5114/amsad.2018.76826.
39. Vásquez Vélez IC, Charris Domínguez CM, Fernández Sánchez MJ, Garavito-Aguilar ZV. Hypoxia and Tissue Regeneration:

Adaptive Mechanisms and Therapeutic Opportunities. Int J Mol Sci. 2025 Sep;26(19):9272. PMID: 41096544. Available from: https://doi.org/10.3390/ijms26199272.

40. Yan W, Chen Y, Yao Y, Zhang H, Wang T. Increased invasion and tumorigenicity capacity of CD44+/CD24- breast cancer MCF7 cells in vitro and in nude mice. Cancer Cell Int. 2013 Jun;13(1):62. PMID: 23799994. Available from: https://doi.org/10.1186/1475-2867-13-62.
41. Canhasi L, Tina E, Eremo AG. Hypoxia-mimetic by $CoCl_2$ increases SLC7A5 expression in breast cancer cells in vitro. BMC Res Notes. 2023 Dec;16(1):366. PMID: 38082346. Available from: https://doi.org/10.1186/s13104-023-06650-2.
42. Sadri M, Delbandi AA, Rashidi N, Kardar GA, Falak R. Cobalt Chloride-induced Hypoxia Can Lead SKBR3 and HEK293T Cell Lines toward Epithelial-mesenchymal Transition. Iran J Allergy Asthma Immunol. 2022 Aug;21(4):449–457. PMID: 36243933. Available from: https://doi.org/10.18502/ijaai.v21i4.10292.
43. Kikuchi D, Minamishima YA, Nakayama K. Prolyl-hydroxylase PHD3 interacts with pyruvate dehydrogenase (PDH)-E1β and regulates the cellular PDH activity. Biochem Biophys Res Commun. 2014 Aug;451(2):288–294. PMID: 25088999. Available from: https://doi.org/10.1016/j.bbrc.2014.07.114.
44. Minh CH, Anh TD, Nguyen S. Effects of $CoCl_2$-Induced Hypoxia on HepG2 Cells: Increased VEGF and GLUT1 Gene Expression and Enhanced Doxorubicin Resistance. VNUHCM Journal of Science and Technology Development. 2025;28(1):3723–3733.
45. Angelé-Martínez C, Murray J, Stewart PA, Haines J, Gaertner AA, Brumaghim JL. Cobalt-mediated oxidative DNA damage and its prevention by polyphenol antioxidants. J Inorg Biochem. 2023 Jan;238:112024. PMID: 36272187. Available from: https://doi.org/10.1016/j.jinorgbio.2022.112024.
46. Hullon D, Ahad A, Dabiry SM, Mahindra L. Cobalt-Induced Cardiomyopathy: Mitochondrial Dysfunction, Oxidative Stress, and Reversible Cardiac Toxicity: A Systematic Review. Cardiovasc Toxicol. 2026 Feb;26(2):24. PMID: 41622383. Available from: https://doi.org/10.1007/s12012-026-10099-7.
47. Cai Y, Li A, Qian Y. Effect of cobalt ions on TNF-α and IL-6 secretion by fibroblasts surrounding hip periprosthetic membrane. Front Bioeng Biotechnol. 2025 Sep;13:1651049. PMID: 41036386. Available from: https://doi.org/10.3389/fbioe.2025.1651049.
48. Wang Y, Zhang L, He M, Chen X, Pei L, Xi S. Cobalt exposure increases fasting plasma glucose by inhibiting hepatic glycogen synthesis and enhancing gluconeogenesis. J Hazard Mater. 2025 Nov;499:140132. PMID: 41106006. Available from: https://doi.org/10.1016/j.jhazmat.2025.140132.
49. Grant MP, Alatassi R, Diab MO, Abushal M, Epure LM, Huk OL, et al. Cobalt ions induce a cellular senescence secretory phenotype in human synovial fibroblast-like cells that may be an early event in the development of adverse local tissue reactions to hip implants. Osteoarthr Cartil Open. 2024 May;6(3):100490. PMID: 38828014. Available from: https://doi.org/10.1016/j.ocarto.2024.100490.
50. Xu X, Zhou T, Tulahong A, Ruze R, Shao Y. Exploring the effects of hypoxia and reoxygenation time on hepatocyte apoptosis and inflammation. PLoS One. 2024 Nov;19(11):e0310535. PMID: 39570857. Available from: https://doi.org/10.1371/journal.pone.0310535.
51. Hunt M, Torres M, Bachar-Wikstrom E, Wikstrom JD. Cellular and molecular roles of reactive oxygen species in wound healing. Commun Biol. 2024 Nov;7(1):1534. PMID: 39562800. Available from: https://doi.org/10.1038/s42003-024-07219-w.
52. Nisar H, Konda B, Hoffmann MD, Labonté FM, Arif M, Diegeler S, et al. Effect of Reoxygenation on Radioresistance of Chronically Hypoxic A549 Non-Small Cell Lung Cancer (NSCLC) Cells Following X-Ray and Carbon Ion Exposure. Int J Mol Sci. 2025 Sep;26(18):9153. PMID: 41009714. Available from: https://doi.org/10.3390/ijms26189153.
53. Nimalasena S, Anbalagan S, Box C, Yu S, Boult JK, Bush N, et al. Tumour reoxygenation after intratumoural hydrogen peroxide (KORTUC) injection: a novel approach to enhance radiosensitivity. BJC Rep. 2024 Oct;2(1):78. PMID: 39391329. Available from: https://doi.org/10.1038/s44276-024-00098-y.
54. Song D, Beringhs AO, Zhuang Z, Joshi G, Tran TH, Claffey KP, et al. Overcoming hypoxia-induced chemoresistance to cisplatin through tumor oxygenation monitored by optical imaging. Nanotheranostics. 2019 May;3(2):223–235. PMID: 31183316. Available from: https://doi.org/10.7150/ntno.35935.
55. Ho YJ, Thao DT, Yeh CK. Overcoming Hypoxia-Induced Drug Resistance via Promotion of Drug Uptake and Reoxygenation by Acousto-Mechanical Oxygen Delivery. Pharmaceutics. 2022 Apr;14(5):902. PMID: 35631488. Available from: https://doi.org/10.3390/pharmaceutics14050902.
56. Lee J, Matienzo ME, Lim S, Evallo E, Kim Y, Jang S, et al. Distinct HIF1α and HIF2α functions control skeletal muscle metabolism and erythropoiesis. J Clin Invest. 2026 Feb;p. e195411. PMID: 41701958. Available from: https://doi.org/10.1172/JCI195411.
57. Shih HM, Pan SY, Wu CJ, Chou YH, Chen CY, Chang FC, et al. Transforming growth factor-β1 decreases erythropoietin production through repressing hypoxia-inducible factor 2α in erythropoietin-producing cells. J Biomed Sci. 2021 Nov;28(1):73. PMID: 34724959. Available from: https://doi.org/10.1186/s12929-021-00770-2.
58. Belkahla S. Dichloroacetate enhances Chemo-sensitivity in wild-type P53 breast cancer cells by modulating ABCG2 and NKG2DL. Sci Rep. 2025 Aug;15(1):29447. PMID: 40789868. Available from: https://doi.org/10.1038/s41598-025-13608-w.
59. Kouhestani SD, Khalili S, Razi A, Aghili M, Moghadam MF. Ectopic expression of miR-34a/-328 sensitizes breast cancer stem cells to gamma rays/doxorubicin by BCL2/ABCG2 targeting. Mol Biol Rep. 2025 May;52(1):490. PMID: 40402331. Available from: https://doi.org/10.1007/s11033-025-10581-5.
60. Yahya SM, Salem SM, Nabih HK, Mohamed SI, Elsayed GH. The miRNA-4330/ABCG2 axis overcomes drug resistance and cancer progression in both ER-positive and ER-negative resistant breast cancer cells. Clin Transl Oncol. 2026 Jan;PMID: 41528714. Available from: https://doi.org/10.1007/s12094-025-04138-y.
61. Zihlif M, Hameduh T, Bulatova N, Hammad H. Alteration in the expression of the chemotherapy resistance-related genes in response to chronic and acute hypoxia in pancreatic cancer. Biomed Rep. 2023 Oct;19(6):88. PMID: 37901880. Available from: https://doi.org/10.3892/br.2023.1670.
62. Francois LN, Gorczyca L, Du J, Bircsak KM, Yen E, Wen X, et al. Down-regulation of the placental BCRP/ABCG2 transporter in response to hypoxia signaling. Placenta. 2017 Mar;51:57–63. PMID: 28292469. Available from: https://doi.org/10.1016/j.placenta.2017.01.125.
63. Mughis H, Lye P, Imperio GE, Bloise E, Matthews SG. Hypoxia modulates P-glycoprotein (P-gp) and breast cancer resistance protein (BCRP) drug transporters in brain endothelial cells of the developing human blood-brain barrier. Heliyon. 2024 Apr;10(9):e30207. PMID: 38737275. Available from: https://doi.org/10.1016/j.heliyon.2024.e30207.